Generation of microwave pulses from the static electric field of a capacitor array by an underdense, relativistic ionization front*

P. Muggli,[†,a)] R. Liou, C. H. Lai, J. Hoffman, and T. C. Katsouleas
Department of Electrical Engineering–Electrophysics, University of Southern California, Los Angeles, California 90089

C. Joshi
Department of Electrical Engineering, University of California Los Angeles, Los Angeles, California 90095

(Received 18 November 1997; accepted 16 January 1998)

The dc to ac radiation converter is a new device in which a relativistic ionization front directly converts the static electric field of an array of alternatively biased capacitors into a pulse of tunable radiation. In a proof-of-principle experiment frequencies between 6 and 21 GHz were generated with plasma densities in the 10^{12} cm^{-3} range and a capacitor period $2d=9.4$ cm. In the present experiment, short pulses with frequencies between 39 and 84 GHz are generated in a structure with $2d=2$ cm. The frequency spectra of these pulses are measured using a diffraction grating. The spectra are discrete, and their center frequency varies linearly with the gas pressure prior to ionization (or plasma density), as expected from theory. Their relative spectral width is around 18%, consistent with the expected number of cycles (six) contained in the pulses. An upper limit of 750 psec (bandwidth detection limited) is placed on the pulses length. The emitted frequency increases from 53 to 93 GHz when the capacitors are connected by pair to obtain a effective array period of 4 cm. © *1998 American Institute of Physics.* [S1070-664X(98)92405-3]

I. INTRODUCTION

Two classes of radiation sources have proven to be extremely successful in producing high-power and/or high-frequency radiation. The first class uses emission from free electron beams to produce electromagnetic (EM) radiation from the microwave frequency range to the infrared (IR) (klystrons, gyrotrons, free electron lasers, masers,...) and even vacuum ultraviolet (VUV) (synchrotrons). The second class uses transitions between atomic or molecular states to produce EM radiation from IR to the VUV (lasers). Recently, alternate sources that directly convert static electric fields into EM radiation have been successfully tested in vacuum devices[1] and in photoswitched semiconductors.[2] In addition, laser-produced ionization fronts have been used to upshift the frequency of an existing radiation source[3] from 35 GHz to more than 150 GHz by a mechanism described as phase modulation in a time-varying medium,[4] or photon acceleration.[5]

In the new device,[6] the radiation is produced through conversion of the static ($\omega_0=0$) electric field from an array of alternatively biased capacitors of period $2d$ (wave number $k_0=\pi/d$) by a laser-produced, underdense, relativistic ionization front. Each time the front crosses a capacitor it triggers a burst of current and, consequently, a burst of broadband radiation. The bursts from each capacitor sum coherently with a phase determined by the front velocity to produce an EM radiation pulse in the plasma with a particular frequency and propagation direction. Since the wave train (ac) that exits the plasma is similar to the waveform of the static (dc) electric field, we refer to this device as a dc to ac Radiation Converter or DARC source. The energy carried by the EM pulse is taken from the electrostatic energy of the capacitor array. The laser pulse energy is used for the ionization of the working gas only. The frequency of the EM pulse is tunable by adjusting either the plasma density (i.e., the working gas pressure prior to ionization) or the capacitor spacing d. In principle, the pulse can be completely tailored for a specific application by modulating the distance between the capacitors along the array (frequency chirping), and by adjusting the voltage applied to each capacitor (temporal shape). The number of cycles of radiation is equal to half the number of capacitors in the array, and the device can produce very short (few cycles) EM pulses. By choosing the capacitor period d and the appropriate plasma density the device can be operated from the microwave to the IR or teraherz frequency range. Applications for a high-power, tunable, ultrashort pulse source ranges from advance radar and remote sensing to ultrafast chemical and biological imaging, ultrafast interaction in solids, atomic physics, etc.

Beside the EM mode excited in the plasma that is the main focus of this paper, a zero-frequency magnetic mode, the free-streaming or picket-fence mode, is theorized to be excited. This mode has never been observed experimentally, and should be observable in the DARC source. Also a small fraction of the energy is reflected at a very high-frequency ($\omega_R \cong 4\gamma_f^2 k_0 c$) since it experiences a double Doppler frequency upshift upon reflection off the relativistic ($\gamma_f > 1000$) ionization front.

This paper reviews the theory[6] (Sec. II) and the first experimental results[7] obtained with a DARC source with d

*Paper qThpI2-4 Bull. Am. Phys. Soc. **42**, 2062 (1997).
[†]Invited speaker.
[a)]Electronic mail: muggli@ee.ucla.edu

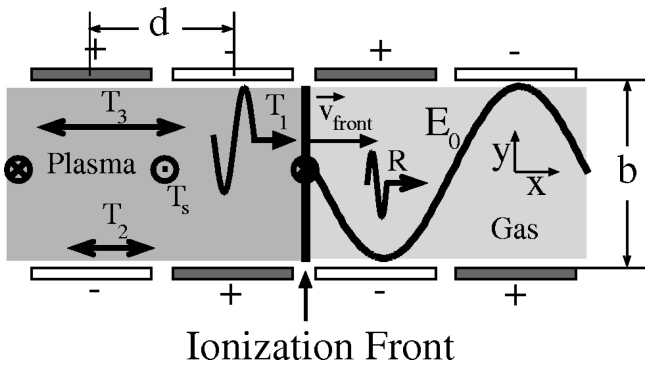

FIG. 1. Geometry of the DARC source. The static electric field of the capacitor array (E_0 ahead of the ionizing laser pulse) is converted into frequency tunable radiation upon transmission through the ionization front. In this diagram (macrostructure), the radiation pulse (labeled T_1) follows the ionization front. The other modes excited at the boundary are the reflected mode (R), two plasma modes (T_2 and T_3), and the free-streaming mode or the picket-fence mode (T_s).

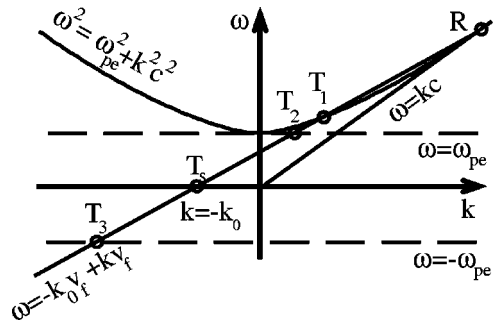

FIG. 2. Dispersion curves (ω-k diagram) for the different modes existing in the DARC source. The modes excited at the ionization front are the tunable radiation (T_1), the plasma modes (T_2, T_3), the free-streaming mode (T_s), and the reflected wave (R). Their frequencies and wave numbers can be obtained from this diagram.

$=4.7$ cm which produced radiation between 6 and 21 GHz (Sec. III A). Section III B describes new experimental results obtained with a Ka-band device ($d=1$ cm) that illustrate unique features of the device, including the production of ultrashort microwave pulses (<750 psec) and broad tunability (e.g., 39–84 GHz) with relatively narrow bandwidth spectrum ($\approx 18\%$), consistent with the number of cycles expected in the pulse (six). Other DARC sources that will be tested in the near future are described in Sec. IV. A summary is given in Sec. V.

II. THEORY

The geometry of the DARC source is shown in Fig. 1. In a simple one-dimensional (1-D) description the electric field between the alternatively biased capacitor plates is of the form $\mathbf{E}=E_0 \sin(k_0 x)\mathbf{y}$, where $k_0=\pi/d$ and d is the distance between adjacent capacitors (see Fig. 1). The structure is filled with a working gas and an ionization front is created by a short laser pulse ($\tau_L < d/c$, c the speed of light) traveling through the structure from left to right. The velocity of the ionization front v_f is equal to the group velocity of the laser pulse (of frequency ω_L) in the ionized gas: $v_f=c(1-\omega_{pe}^2/\omega_L^2)$, where $\omega_{pe}^2=n_e e^2/\varepsilon_0 m_e$ is the plasma frequency in the plasma of density n_e left behind the ionization front. In general $\omega_L \gg \omega_{pe}$, $v_f \cong c$, and the front's relativistic factor is large $\gamma_f=(1-v_f^2/c^2)^{1/2} \cong \omega_L/\omega_{pe} \gg 1$. To derive the frequency of the radiation generated (EM wave transmitted through the front into the plasma), consider the situation in a frame moving with the ionization front. The Lorenz transformed electrostatic field of the capacitor array approximates an electromagnetic wave ($v_f \cong c$) with frequency $\omega'=k_0 v_f \cong k_0 c$ and $B_0'=E_0'/v_f \cong E_0'/c$ (the primed quantities are in the front's frame). In the front's frame the EM wave of frequency $\omega'=\gamma_f k_0 v_f$ is incident in the $-\mathbf{x}$ direction upon the ionization front which is static at $x=0$, and gives rise to a reflected wave (moving in the $+\mathbf{x}$ direction), and to a transmitted wave (moving in the $-\mathbf{x}$ direction) into the plasma. All these EM waves are at the same frequency ω'. The EM wave transmitted into the plasma is the tunable radiation that is the primary subject of this paper. In the plasma it satisfies the usual dispersion relation: $\omega'^2=\omega_{pe}^2+k_0'^2 c^2$; ω_{pe} is a Lorenz invariant. Transforming back into the laboratory frame the frequency of the EM wave that exits the plasma is given by[6]

$$\omega=\gamma_f^2 k_0 v_f\left[1-\frac{v_f}{c}\left(1-\frac{\omega_{pe}^2}{\gamma_f^2 k_0^2 v_f^2}\right)^{1/2}\right]. \tag{1}$$

When $\omega' \gg \omega_{pe}$, namely $\omega_L \gg \omega_{pe}^2/k_0 v_f$, Eq. (1) can be approximated by

$$\omega \cong \frac{k_0 v_f}{2}+\frac{\omega_{pe}^2}{2k_0 v_f}. \tag{2}$$

For a given plasma density Eq. (2) has a minimum for $k_{0,\min}=\omega_{pe}/v_f$. Structures with $k_0 > k_{0,\min}$ are called microstructures. Structures with $k_0 < k_{0,\min}$ are called macrostructures and are used in the experiments described in this paper. For a given k_0, frequency tuning is achieved by changing the plasma density [Eq. (2)], i.e., the neutral gas density prior to ionization. The frequency produced by the DARC source varies linearly with the plasma density n_e.

The frequency of the transmitted EM wave can also be obtained in the laboratory frame from the continuity of the phase of the different waves at the moving boundary (ionization front). The phase of the ''incident wave'' is given by $-k_0 x$ (static field, $\omega_0=0$), while the phase of the transmitted wave is given by $\omega t-kx$, where ω and k satisfy $\omega^2=\omega_{pe}^2+k^2c^2$. Equating the phases at $x=v_f t$ and substituting for k gives the result in Eq. (1). Dispersion curves for the modes at play in the DARC source are plotted in Fig. 2 for the macrostructure case. The frequency and wave number of the transmitted mode are obtained from the intersection (labeled T_1 in Fig. 2) of the EM wave in the plasma with the straight line of slope $\omega/k=v_f$ passing by $k=-k_0$. The EM mode is generated with positive phase and group velocities, which indicates that the EM pulse follows the ionization front ($v_f > 0$) and exits the source on the same side as the laser pulse exits. Since the actual electric field generated by the capacitors has an $\mathbf{x}$ component (2-D field), coupling to electrostatic plasma modes (labeled T_2 and T_3 in Fig. 2) also occurs. Assuming that the electron–ion pairs are created at rest by the ionization process (i.e., $\mathbf{j}=0$ and $\rho=0$ at the boundary

$x=v_f t$), a fourth plasma mode (labeled T_s in Fig. 2), called the free-streaming or picket-fence mode, is also excited. It consists of a static ($\omega_s=0$) magnetic field, perpendicular to the capacitors electric field, with a direction alternating in space with the same periodicity $2d$ as the static electric field (see Fig. 1). This mode is sustained by the steady currents flowing between the capacitor plates. In the case where $\Delta \ll k_0$ the static electric field of the capacitor array can be expanded as[6]

$$\begin{aligned} E_y &= \sum_{n=0}^{\infty} \frac{(-1)^n 2k_0 V_0}{\pi \sinh([2n+1]k_0 b/2)} e^{i(2n+1)k_0 x} \\ &\quad \times \cosh([2n+1]k_0 y), \\ E_x &= \sum_{n=0}^{\infty} \frac{i(-1)^n 2k_0 V_0}{\pi \sinh([2n+1]k_0 b/2)} e^{i(2n+1)k_0 x} \\ &\quad \times \sinh([2n+1]k_0 y), \end{aligned} \tag{3}$$

where the origin is placed in the middle of one of the capacitors, and V_0 is the total voltage applied to the capacitors. Near the axis, the first term ($n=0$, amplitude E_0) in the sum is approximately equal to V_0/b, is always the largest by a factor 3 or more, and is the only one retained in the following analysis. To ensure the continuity of the fields everywhere along the boundary, all the modes are assumed to have the same spatial characteristics as the static field [Eq. (3)]. The sinh and cosh terms Fourier decompose into an infinite number of k_y components, and because of the dispersion relation for the transverse modes ($\omega^2=\omega_{pe}^2+k_x^2c^2+k_y^2c^2$), each k_y component would lead to a different ω and k_x. However, for large upshift ($\omega_{pe}\gg k_0 c$) the $k_y^2c^2$ term (of order $k_0^2c^2$) in the dispersion relation can be neglected, and the transmitted mode can be considered as having a single frequency. To obtain the amplitudes of the fields for the five modes (R, T_1, T_2, T_3, T_s) the boundary conditions for the fields have to be solved in the front's frame and the results transformed back into the laboratory frame. For a large upshift ($\omega_{pe}/k_0 c\gg 1$) and a relativistic ionization front ($v_f \cong c$) they are approximated by

$$\begin{aligned} T_1 &\cong 1+2(k_0 c/\omega_{pe})^2, \\ T_2 &\cong -k_0 c/2\omega_{pe}(1+2k_0 c/\omega_{pe}), \\ T_3 &\cong -k_0 c/2\omega_{pe}\times(1+2k_0 c/\omega_{pe}), \\ T_s &\cong -1, \\ R &\cong (2\omega_{pe}/\gamma_f \beta_f k_0 c)^2. \end{aligned} \tag{4}$$

Thus the amplitude of the electric field of the transmitted EM wave is approximately equal to that of the static electric field E_0 of the capacitors ($T_1\cong 1$). Note that T_s is defined as cB_s/E_0. With an array of N capacitors the output pulse is $N/2$ cycles long, i.e., its time duration is $\tau=N\pi/\omega$, and its bandwidth scales as $\Delta\omega/\omega\approx 2/N$ and depends on the particular pulse shape. Assuming that the plasma completely shields the capacitors field, the energy carried by the output pulse is given by

$$W=\frac{1}{2}\sqrt{\frac{\varepsilon_0}{\mu_0}}\frac{N\pi A}{\omega}T_1^2E_0^2, \tag{5}$$

where A is the spot area of the ionizing laser pulse ($A\leqslant a\times b$ the waveguide cross area). The output power is given by

$$P_{\text{out}}=\frac{W\omega}{N\pi}=\frac{1}{2}\sqrt{\frac{\varepsilon_0}{\mu_0}}AT_1^2E_0^2. \tag{6}$$

The efficiency of the device η, defined as the ratio of the energy in the output pulse to the electrostatic energy stored in the ionized volume, is given by

$$\eta=\frac{1}{2}\frac{k_0 c}{\omega}T_1^2. \tag{7}$$

For large upshift ($\omega\gg k_0 c$, $T_1\approx 1$), the efficiency tends toward $\eta\approx\lambda/d\approx 4k_0^2c^2/\omega_p^2$. The energy of the laser pulse is not included in η. The above analysis is valid only for sharp fronts [i.e., front spatial extend much less than $(\gamma_f^2 k_0)^{-1}$]. A WKB analysis shows that the results for the transmitted mode remain the same for continuous fronts.[6] The sharpness of the ionization front depends on the ionizing laser pulse length and on the ionizing process.

III. EXPERIMENTAL RESULTS

A. Large structure

The large structure consists of $N=12$ capacitors $a=4.1$ cm wide with $b=1.5$ cm, $d=4.7$ cm, and the gap between capacitors is $\Delta=0.6$ cm. The working gas is azulene (C_8H_{10}, ionization potential 7.42 eV), and azulene vapor of a few millitorrs is obtained by sublimation of azulene crystals around 100 °C. Two photon ionization by a 50 psec, 30 mJ, 8 mm in diameter ultraviolet ($\lambda_L=266$ nm) laser pulse yields to plasma densities in the 1×10^{11} to 5×10^{12} cm^{-3} range. For a fixed laser pulse intensity, the plasma density is expected to be linearly proportional to the initial azulene vapor pressure. The plasma density n_e is calibrated versus the azulene vapor pressure (for a fixed laser pulse intensity) by interferometry at 60 GHz in a Q-band waveguide vacuum system. The calibration is 5.1×10^{11} cm^{-3}/mT of azulene with 30 mJ of UV energy. A dc high voltage (HV) between 300 and 1000 V is applied to the capacitors. With these experimental parameters, Eq. (2) predicts that frequencies in the 10 GHz range should be produced. At these frequencies the capacitor array dimensions (a and b) are comparable to the wavelengths of the radiation generated ($\lambda\approx 3$ cm). The waveguide effect of the array can be taken into account in Eq. (2) [or Eq. (1)] by assuming that only one TE mode propagates in the structure:

$$\begin{aligned} \omega &\cong \frac{k_0 v_f}{2}+\frac{\omega_{c,mn}^2}{2k_0 v_f}+\frac{\omega_{pe}^2}{2k_0 v_f} \\ &\cong \frac{1}{2k_0 c}(k_0^2c^2+\omega_{c,mn}^2+\omega_{pe}^2), \end{aligned} \tag{8}$$

where $\omega_{c,mn}=c[(n2\pi/a)^2+(m2\pi/b)^2]^{1/2}$ is the cutoff frequency for the TE_{mn} mode in the waveguide of transverse

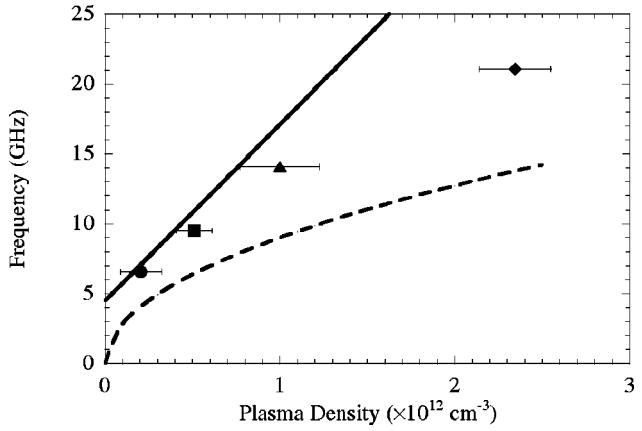

FIG. 3. Frequency generated by the large DARC source ($d=4.7$ cm), as measured with the cutoff waveguide technique versus plasma density. The experimental points are obtained with detection systems in the X-band ($f_c=6.560$ GHz, circle), Ku-band ($f_c=9.490$ GHz, square), K-band ($f_c=14.080$ GHz, triangle), and Ka-band ($f_c=21.100$ GHz, diamond). The line dashed is the plasma frequency and the continuous line is the frequency expected from the DARC source according to Eq. (8) for the TE_{10} mode.

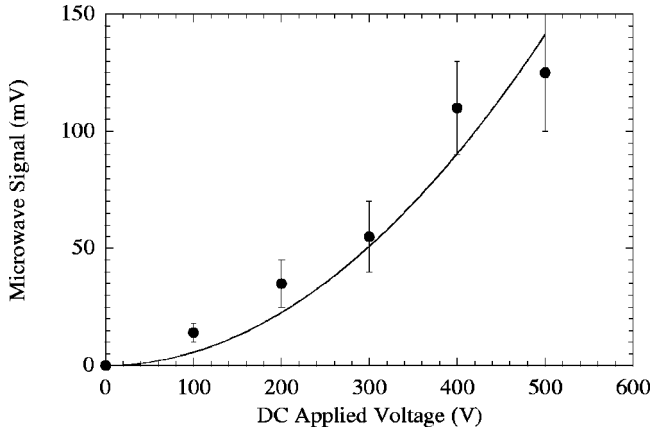

FIG. 4. Intensity of the microwave signal as a function of the applied voltage V_0, detected by an X-band diode at an azulene pressure of 1 mT ($n_e=1\cdot10^{12}$ cm^{-3}), corresponding to a frequency of around 10 GHz (see Fig. 3). The line is the best fit to a $P\propto V_0^2$ dependency predicted by Eq. (6).

dimensions a and b. The waveguide slows down the wave generated and increases its frequency (for a given plasma density), in agreement with the general frequency upshifting theory.[6] Experimentally, the frequency is measured using the cutoff waveguide technique. Starting from zero azulene pressure, the laser is fired while observing the signal on a microwave diode placed after a section of waveguide, and a horn, all in a given band. For pressures (and thus plasma densities) such that the frequency generated is lower than the cutoff frequency (f_c) of the fundamental TE_{10} mode of the rectangular waveguide, no signal is observed. When the pressure gives rise to a frequency approximately equal to the cutoff frequency, an onset of the signal is observed on the microwave diode as a function of the gas pressure. The signal reaches a plateau for slightly higher pressures. Figure 3 shows the plasma densities at which the signal onset has been observed on the X-, Ku-, K-, and Ka-band diodes. Also plotted are the plasma frequency and the frequency expected from the DARC source according to Eq. (8), assuming the radiation propagates in the TE_{10} mode. The three lower frequency data points are in good agreement with the theory [Eq. (8)]. Azulene is an organic molecule and the absorbed UV photons may not necessarily lead to the ionization of the molecule. This translates into a relatively large photon absorption ($>10\%$ over a 60 cm length at 1 mT), but corresponds to a small fractional ionization ($<1.5\%$). At a pressure of 5 mT, corresponding to the onset of the highest frequency data point on Fig. 3, only 10% of the incident UV energy is transmitted through the structure. The plasma density decreases along the structure, and is on average lower than that expected from the calibration. As a result the measured frequency is lower than that predicted by Eq. (8). Error bars in Fig. 3 correspond to the pressure range over which the onset occurred. Figure 3 demonstrates that with this DARC source continuously tunable radiation between 6 and 21 GHz can be produced.[7] The amplitude of the signal detected by an X-band microwave diode is plotted in Fig. 4 as a function of the dc applied voltage and follows the V_0^2 ($V_0\cong E_0\cdot b$) dependency predicted by Eq. (6). Calibration of the microwave diode leads to maximum power levels of a few hundred milliwatts. Equation (6) predicts power levels of a few hundred watts for the maximum applied voltage. Cold test measurements indicate that the output coupling efficiency of the structure is of the order of -30 dB or less and could account for the low output power levels measured in the experiment.

B. Ka-band structure

In the Ka-band structure, the capacitor array consists of $N=12$ capacitors with a period $d=1$ cm. The capacitor plates are separated by $b=0.3556$ cm and are $a=2b$ wide (Fig. 5). The side walls are kept continuous along the structure and the a and b dimensions correspond to those of a Ka-band waveguide. All the dc breaks are $\Delta=0.0635$ cm wide in order to minimize HV breakdown. Pulsed HV ($\approx$300 ns full width at half-maximum, up to 6 kV peak voltage) is applied alternatively to the top or bottom plate of the capacitors, while the other plate and the continuous side wall are kept at ground potential. The working gas is TMAE [Tetrakis(dimethylamino)ethylene or $C_{10}H_{24}N_4$, ionization potential 5.36 eV] an organic liquid that is ionized through two-photon photoionization by the 266 nm laser pulse (4.68 eV photons). The TMAE has a relatively high vapor pressure at room temperature (boiling point 59°) and no energy deple-

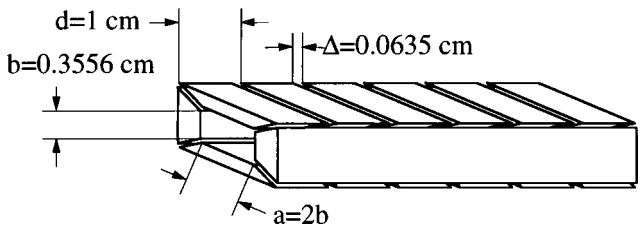

FIG. 5. Schematic of the capacitor array that forms the slotted Ka-band waveguide, and its relevant dimensions. Only six capacitors are shown; the real structure has $N=12$ capacitors. The side wall of the waveguide is kept continuous, whereas the top and bottom walls are cut into capacitor plates.

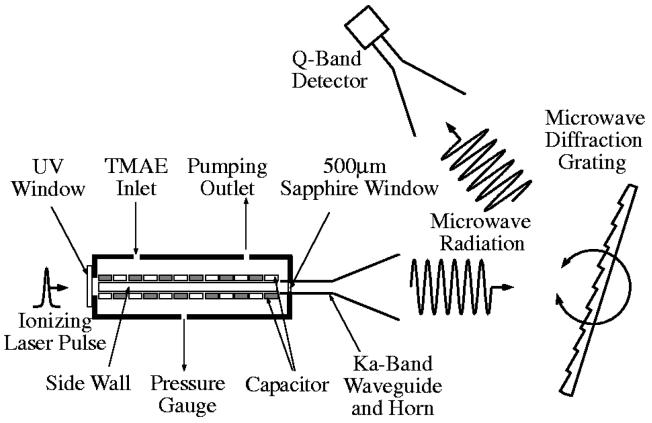

FIG. 6. Experimental setup for the frequency spectra measurements above 30 GHz. The angle between the emitting horn and the receiving horn is kept constant while the grating is rotated.

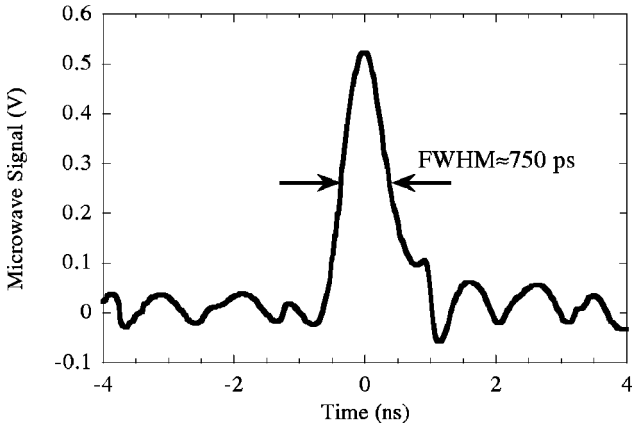

FIG. 7. The microwave signal detected by the microwave diode observed on a 1-GHz bandwidth oscilloscope. The FWHM is about 750 ps and is detection bandwidth limited. $P_{\mathrm{TMAE}}=14$ mT, $V_0=5.3$ kV, $f\cong 65$ GHz, $N=12$; theory predicts that the pulse duration should be $\pi N/\omega\cong 93$ ps.

tion of the UV laser beam has been observed at pressures up to 1 Torr. The voltage the structure can withstand without breakdown decreases with increasing TMAE pressure and ultimately limits the frequencies [Eq. (8)] and powers ($\approx V_0^2$) reachable in this experiment. According to Eq. (8) frequencies above the Ka-band cutoff frequency (21.10 GHz) can be generated with plasma densities higher than $1.551.55\times 10^{12}$ cm^{-3} (assuming propagation in the TE_{10} rectangular mode). The frequency spectrum of the radiation generated with a given plasma density is measured using a microwave grating consisting of 50 6.64-mm grooves and blazed with a 30° angle. The incident wave is *s*-polarized and the signal is observed in the $m=-1$ or $m=-2$ reflection orders. For a grating with a blazing angle of 26°45′, the reflection efficiency is strongly reduced[8] for $m\lambda/d<0.7$, i.e., for frequencies larger than 64.5 GHz in the $m=-1$ order with a groove spacing of 6.64 mm. Thus in this experiment (blazing angle of 30°) frequencies above 60 GHz are observed in the $m=-2$ order. A waveguide and detection diode with the appropriate cutoff frequency are used to ensure that the signals observed at large incidence angle are really second-order reflections. The angle between the emitting and the receiving horn is kept constant (15°) while the grating is rotated to acquire the frequency spectrum (see Fig. 6). The microwave signal is detected using a DXP-22 millitech® diode (*Q*-band) and a 1 GHz bandwidth scope or digitizer connected to a computer-controlled data acquisition system. The spectrum is constructed from multiple shots taken at different angles of incidence on the grating. Cold test measurements with a Ka-band frequency sweeper show that the resolution of the frequency measurement system is 4 GHz between 26.5 and 40 GHz. This value is in agreement with the value obtained from the grating equation ($\partial f/\partial\theta$) times the equivalent horns/grating collection angle ($\Delta\theta\cong 6°$). The resolution can thus be calculated for larger incident frequencies for which no cold test is performed and is found to be around 12 GHz at 60 GHz. Note that observing higher frequencies in the $m=-2$ order preserves the good resolution ($\Delta f/f\leqslant 10\%$) measured up to 40 GHz.

Figure 7 shows the microwave signal when reflected from the back of the grating (acting as a plane mirror with a 7.5° incidence angle). The full width at half-maximum (FWHM) of the signal is 750 psec, and is bandwidth limited by the RC time constant of the microwave diode, cable, and oscilloscope ($\cong 1$ GHz bandwidth). At this TMAE pressure ($P_{\mathrm{TMAE}}=14$ mT), the pulse center frequency is expected to be about 65 GHz (see Fig. 10) with a pulsewidth of $\pi N/\omega\cong 93$ psec. (Similar signals were obtained over the whole frequency range of Fig. 10.) To our knowledge these are the shortest pulses in this frequency range.[9] Figure 8 shows the frequency spectrum of the radiation measured at TMAE pressures of 2, 5, and 24 mT, leading to center frequencies of 39 and 53, (observed in the $m=-1$ order), and 84 GHz (observed in the $m=-2$ order), respectively. These spectra are discrete and their relative spectral width $\Delta\omega/\omega$ defined as the ratio of the FWHM to their center frequency, together with the width of spectra obtained at 8 and 12 mT (not

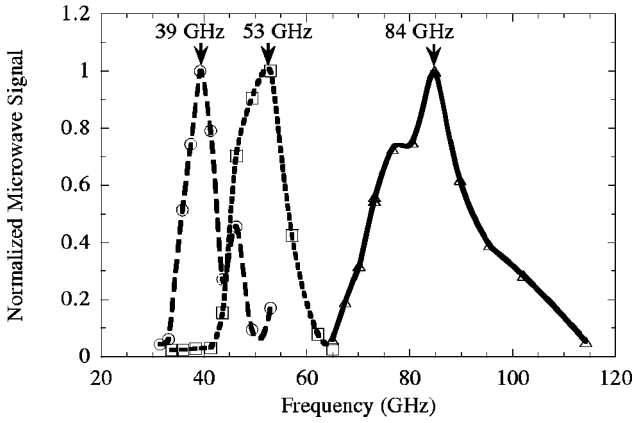

FIG. 8. Frequency spectra obtained at 2 mT (circles and long-dash line), 5 mT (squares and short-dash line), and 24 mT (triangles and continuous line) of TMAE pressure. The lines are added to guide the eyes. The spectra are obtained by observing the signal reflected in the $m=-1$ (2 and 5 mT) and $m=-2$ order (24 mT) of a microwave grating with 50 6.64-mm grooves blazed with a 30° angle. The spectra are normalized to their peak value. The center frequencies are 39, 53, and 84 GHz, and their respective FWHM are 7.0 GHz (18%), 10.9 GHz (20%), and 19.6 GHz (23%). The frequency resolution is about 4 GHz or 10% between 26 and 40 GHz both in the first and second reflection order.

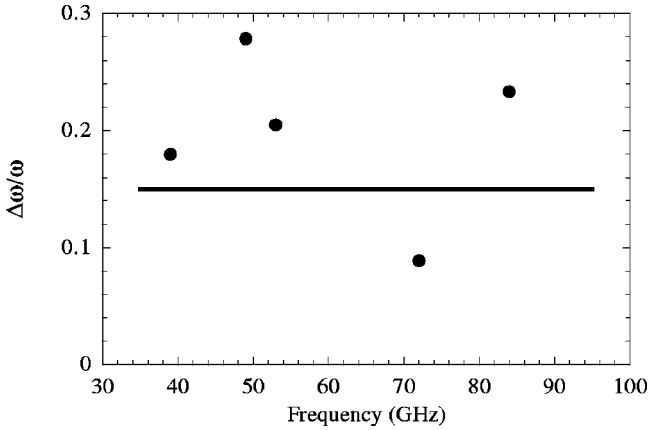

FIG. 9. Relative spectral width of the spectra measured at different TMAE pressures 2, 5, 8, 12, and 24 mT versus the spectra central frequency. The continuous line is the value expected for a pulse with $N/2=6$ cycles: $\Delta\omega/\omega\cong 2/N\cong 15\%$.

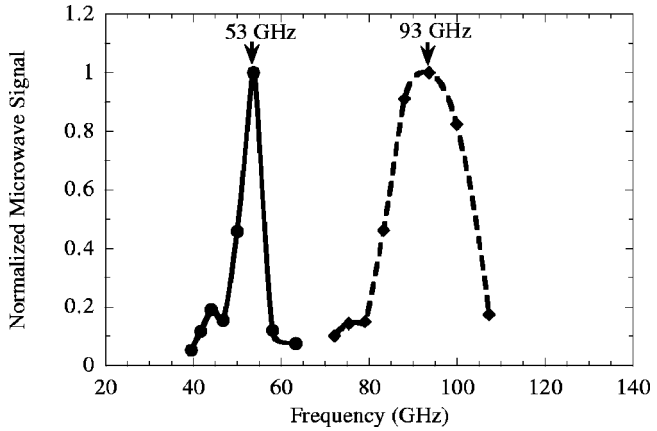

FIG. 11. Frequency spectra obtained with the 12 capacitors connected alternatively, i.e., with a period $2d$ and $N/2=6$ cycles (circles, continuous line), and with the capacitors connected by pairs, i.e., with an effective period $4d$ and $N/2=3$ cycles (diamonds, dashed line). The lines are added to guide the eyes. The center frequencies are 53 and 93 GHz, and the FWHM are 8 GHz (15%) and 21 GHz (23%), respectively.

shown), is plotted on Fig. 9. The relative spectral widths are consistent with the expected width of $N/2=6$ cycles pulses: $\Delta\omega/\omega=2/N\cong 15\%$. The shape and the width of the frequency spectra (see Fig. 8) and thus the time shape of the pulses are affected by the frequency-dependent distributed losses introduced by the dc breaks. The frequency versus TMAE pressure as measured with the grating system and a cutoff wave guide is plotted in Fig. 10. An estimate for the plasma densities necessary to produce the observed frequencies is obtained from the best linear fit of Fig. 10 and yields a TMAE pressure to plasma density conversion factor of 7.12×10^{11} cm^{-3}/mT of TMAE, corresponding to an ionization fraction around 2%. The plasma density was measured for the same laser intensity in a U-band waveguide interferometer at 60 GHz described in Ref. 3, and the conversion factor obtained was 4.63×10^{11} cm^{-3}/mT of TMAE. The discrepancy between these two numbers is not understood at this point but will be further investigated. The fit on Fig. 10 crosses the $P_{\mathrm{TMAE}}=0$ axis at a frequency of 39 GHz instead of the 22.31 GHz obtained from Eq. (8) for the TE_{10} mode with $\omega_{pe}=0$. Interferometry traces at $P_{\mathrm{TMAE}}=0$ indicate the creation of a plasma density around 2×10^{12} cm^{-3}, probably caused by ionization of the window surface and by laser beam interception along the waveguide walls. According to Eq. (8) the plasma density necessary to generate 39 GHz radiation is about 5×10^{12} cm^{-3}.

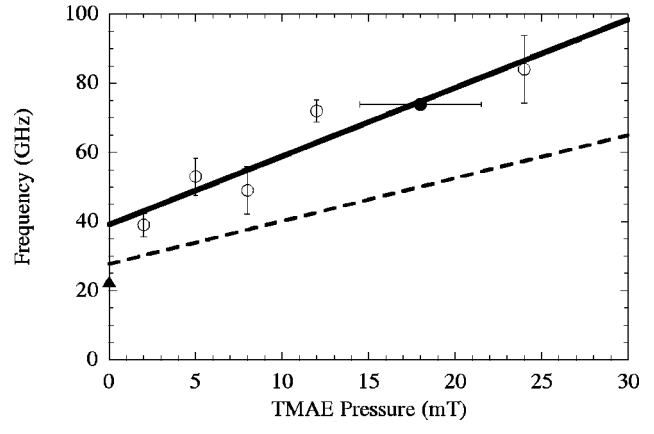

FIG. 10. Frequency versus TMAE pressure as measured with the grating arrangement (open circles), and with the cutoff waveguide method (filled circle). The error bars correspond to the measured FWHM and to the range over signal onset was observed. The spectra are observed in the $m=-1$ order of the grating at 2, 5, and 8 mT, and in the $m=-2$ order of the grating at 12 and 24 mT. The line shows the best linear fit to these data points and corresponds to a plasma density of 7.12×10^{11} cm^{-3}/mT of TMAE. The triangle at $P_{\mathrm{TMAE}}=0$ corresponds to the frequency value obtained from Eq. (8) with $d=1$ cm, $\omega_{pe}^2=0$, and for the TE_{10} mode. Also shown, the frequency that would be obtained if the plasma frequency followed the 4.63×10^{11} cm^{-3}/mT of TMAE calibration (dashed line).

The frequency of the radiation produced by the DARC source can be changed, for a given plasma density, by changing the capacitor array period [Eq. (8)]. In the experiment this is achieved by electrically connecting the capacitors by pairs, i.e., changing d into $2d$. The frequency spectra measured with the $2d$ and $4d$ periods are plotted in Fig. 11. The center frequencies are 53 ($m=-1$) and 93 GHz ($m=-2$), in good agreement with the results of Fig. 10 and Eq. (8). A 7 cm long section of W-band waveguide ($f_c=59.010$ GHz) is used to ensure that the high-frequency signal is in the $m=-2$ reflection order of the grating. The high-frequency spectrum is broader than the low-frequency spectrum, but is narrower than expected for the $N/2=3$ cycles signal.

Figure 12 shows the microwave signal measured at $P_{\mathrm{TMAE}}=15$ mT, as a function of the applied voltage. The signal follows the $P\approx V_0^2$ ($V_0\cong E_0\cdot b$) dependency predicted by Eq. (6). The diode is calibrated with a cw microwave signal at the appropriate frequency. Assuming that for pulses of duration shorter than that given by the detection system bandwidth (corresponding to 750 psec, see Fig. 7) the diode produces signals proportional to the pulse energy, and assuming that the actual pulse duration is that of a six-cycle pulse at the frequency inferred from the TMAE pressure (see Fig. 10), an estimate of the output power level can be obtained from the diode signals. Such an estimate places the maximum signals observed with this structure in the 100 mW range for an applied voltage of 5 kV.

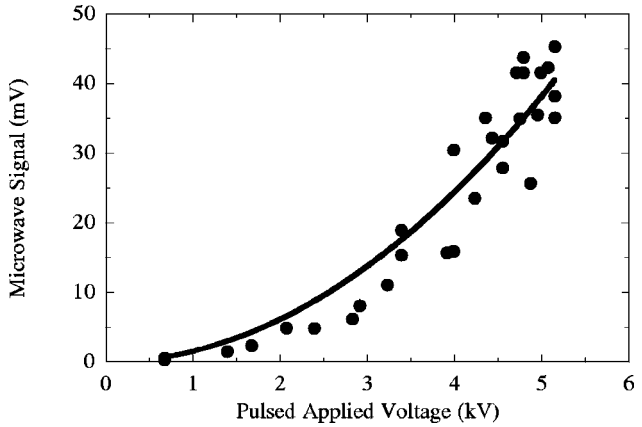

FIG. 12. Microwave signal as a function of the applied voltage V_0 at $P_{TMAE}=15$ mT corresponding to a frequency of around 65 GHz. The line is the best fit to a $P \propto V_0^2$ dependency predicted by Eq. (6).

IV. OTHER DARC SOURCES

When operated in the microwave frequency range, the capacitor array has to act as a waveguide with acceptable transmission characteristics. The sources that were tested so far (see previous paragraph) exhibit relatively poor transmission characteristics in cold tests, which probably accounts for the relatively low power signals measured. The dc breaks of the capacitor array perturb the wall current necessary for the free propagation of the waveguide modes. These structures are essentially capacitor arrays supporting microwave propagation. In order to improve the microwave characteristics of the DARC source, and to take full advantage of the potential high output power of the scheme, a source in the X-band (Fig. 13) has been designed in which the capacitor plates are replaced by pins inserted in the waveguide through small hole in its narrow side wall. Cold test results indicate that the transmission characteristics of this device are those of a plain waveguide, except for stopbands created by the pins periodic structure. For example, the distance between the pins can be chosen such that the first stopband appears outside of the X-band frequency range (8.20–12.40 GHz). Calculations of the electric field pattern inside the waveguide show that the stored energy available for conversion into EM radiation is only a factor of 3 smaller than in the plate case. The output power of this device should thus be much higher than that of the previous devices. This DARC source will be tested in the near future.

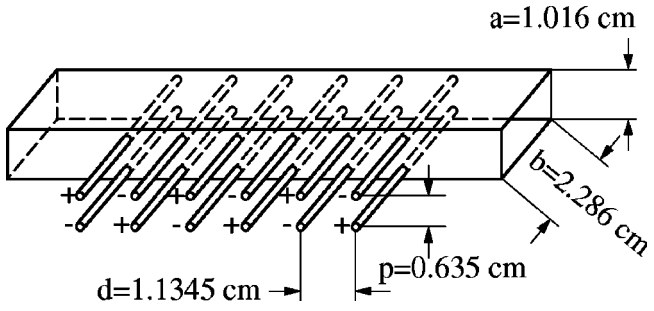

FIG. 13. Schematic of a DARC source in the X-band. The pins introduced through the narrow side wall of the waveguide play the role of capacitors. In cold test the structure exhibits no insertion, except for narrow stopbands created by the periodic pins.

Equations (1) or (2) indicate that a DARC source with a period d of 330 μm produces teraherz radiation with plasma densities in the 10^{17} cm^{-3} range. Such a device has been built and will be operated in the 5–20 μm wavelength range. The plasma density required to produce those short wavelengths will be obtained through field ionization of nitrogen or xenon by a high-intensity femtosecond laser pulse.

V. SUMMARY AND CONCLUSIONS

The DARC source is a new device in which the static electric field of an array of alternatively biased capacitors is directly converted into EM radiation by a laser-produced relativistic ionization front. The results presented in this paper show that microwaves between 6 and 21 GHz and 39 and 93 GHz are produced with two devices with capacitor spacing in the centimeter range ($d=4.7$ and 1.0 cm, period $2d$) and plasma densities in the 10^{12}–10^{13} cm^{-3} range. The radiation frequency can be tuned either by adjusting the plasma density (i.e., gas pressure prior to ionization) or the distance d between the capacitors. The pulses frequency spectra are discrete with a center frequency that varies linearly with the plasma density, and with a relative FWHM around 18%, consistent with their expected number of cycles ($N/2=6$, N is the number of capacitors in the array). The pulses are expected to be extremely short (<200 psec above 30 GHz, Ka-band source), and an upper bound to their width is experimentally placed at 750 psec (detection bandwidth limited). The amplitude of the measured signals follows the V_0^2 dependency (V_0 voltage applied to the capacitors) predicted by theory, but their power level remains lower than expected (in the 100 mW range up to $V_0=5$ kV). Cold test measurements show that the cut in the waveguide necessary for the capacitor array introduces an insertion loss of around -30 dB between 26.5 and 40 GHz (Ka-band) that certainly contributes to the low observed powers. Expression (6) is derive from a plane wave propagation theory. However, in the microwave frequency range the excitation and propagation of the generated radiation should take into account the characteristics of the supporting structure (''waveguide''). A new structure has been built in an X-band waveguide that exhibits no insertion loss between the narrow stopbands introduced by the periodic pins that act as capacitor plates. The issue of the power effectively produced by the DARC source and coupled to a waveguide mode will be better addressed with that structure. The range of frequencies generated by the DARC source will be extended to the terahertz range with a structure with a capacitor spacing of 330 μm and a plasma density around 10^{17} cm^{-3}. Experiments are conducted to detect the never observed free-streaming or picket-fence mode, a zero-frequency magnetic mode that is theoretically excited in the DARC source.

ACKNOWLEDGMENTS

The authors acknowledge useful discussions with Dr. K. Marsh, Dr. C. E. Clayton, and G. Roth.

This work was supported by the Air Force Office for Scientific Research Grant No. F49620-95-1-0248, U.S. Department of Energy Grant No. DE-FG03-92ER-40745, and National Science Foundation Grant No. ECS-9632735.

[1]A. K. Ganguly, P. M. Phillips, and H. F. Gray, J. Appl. Phys. **67**, 7098 (1990).
[2]D. You, R. Jones, P. Bucksbaum, and D. Dykaar, Opt. Lett. **18**, 290 (1993); *Ultrawide-band Short Pulse Electromagnetics*, edited by L. Bertoni, L. Carin, and L. B. Felsen (Plenum, New York, 1993); D. H. Auston, in *Ultrashort Laser Pulses*, edited by W. Kaiser (Springer Verlag, New York, 1993), Chap. 5; M. B. Ketchen, D. Grischkowski, T. C. Chen, I. N. Duling III, N. J. Halas, J.-M. Halbout, J. A. Kash, and G. P. Li, Appl. Phys. Lett. **48**, 24 (1986).
[3]R. L. Savage, R. P. Brogle, W. B. Mori, and C. Joshi, IEEE Trans. Plasma Sci. **21**, 5 (1993); R. L. Savage, W. B. Mori, and C. Joshi, Phys. Rev. Lett. **68**, 946 (1992).
[4]E. Yablonovitch, Phys. Rev. Lett. **31**, 877 (1975); W. M. Wood, C. W. Siders, and M. C. Downer, Phys. Rev. Lett. **67**, 3523 (1991); D. K. Kalluri, IEEE Trans. Plasma Sci. **21**, 77 (1993).
[5]S. C. Wilks, J. M. Dawson, W. B. Mori, T. Katsouleas, and M. E. Jones, Phys. Rev. Lett. **62**, 2600 (1989).
[6]W. B. Mori, T. Katsouleas, J. M. Dawson, and C. H. Lai, Phys. Rev. Lett. **74**, 544 (1995).
[7]C. H. Lai, R. Liou, T. C. Katsouleas, P. Muggli, R. Brogle, C. Joshi, and W. B. Mori, Phys. Rev. Lett. **77**, 4764 (1996).
[8]E. G. Loewen, M. Neviere, and D. Maystre, Appl. Opt. **16**, 2711 (1977).
[9]P. Muggli, R. Liou, J. Hoffman, C. Joshi, and T. Katsouleas, Appl. Phys. Lett. **72**, 19 (1998).